

Fiber-Optic Sensor for Detecting PFAS Compounds in Water Using a Fabry–Pérot cavity

Patryk Radek,* Kamil Barczak, and Aneta Olszewska

Department of Optoelectronics, Silesian University of Technology 44-100 Gliwice,

Received May 16, 2025; accepted June 30, 2025; published June 30, 2025

Abstract—A PVDF-coated Fabry–Pérot fiber-optic sensor was developed for rapid in situ detection of PFAS in water. A low-finesse etalon was formed by dip-coating, yielding interference minima that shift by an average of 5 nm during wet–dry cycling ($SD = 0.7$ nm). Exposure to a 10 $\mu\text{g}/\text{mL}$ PFOS solution induced a reversible 5.9 nm redshift, and subsequent rinsing restored the baseline within 0.4 nm. The sensor's low cost, portability, and high repeatability make it well suited for field applications.

Per- and polyfluoroalkyl substances (PFAS) constitute a vast family of entirely synthetic chemicals, all sharing the presence of exceptionally strong carbon–fluorine (C–F) bonds. The bond dissociation energy of C–F exceeds 488 kJ/mol, making these among the most robust structures in organic chemistry. This extraordinary strength renders PFAS highly resistant to common degradation pathways: they do not undergo oxidation, hydrolysis, or photodegradation under UV exposure [1].

As a result, these compounds retain their integrity even under extreme conditions, temperatures above 400 °C, exposure to strong oxidants, or prolonged sunlight. In practice, this leads to their accumulation in surface waters, groundwater, soils, and sediment layers. Moreover, because PFAS can be transported in both liquid and gaseous phases, they travel vast distances; they have been detected in remote regions of the Arctic and Antarctic, as well as in wildlife living far from anthropogenic sources.

Owing to their resilience and widespread dispersion, PFAS bioaccumulate through food webs, and higher trophic levels exhibit increasing concentrations in tissue. Epidemiological and laboratory studies have linked PFAS exposure to a range of adverse health effects, from hormonal disruption and weakened immunity, through elevated cancer risk, to developmental defects in fetuses and metabolic disorders [2].

In response to mounting evidence of these hazards, numerous countries have imposed restrictions on the production and use of long-chain PFAS (e.g., PFOA, PFOS), while simultaneously accelerating the development of technologies for their detection and removal from water and soil. Effective monitoring has thus become

indispensable both for scientific research and for environmental and public-health policy.

Furthermore, there is an urgent need for modern PFAS detection systems, since traditional analytical techniques liquid and gas chromatography coupled with mass spectrometry though highly precise, are time-consuming, costly, and require complex sample preparation and specialized personnel. Their inability to perform in situ measurements or real-time monitoring further limits their utility in rapid-response scenarios. New sensor technologies, particularly those based on fiberoptic techniques, offer the potential for rapid, low-cost, and reproducible field measurements with high sensitivity and selectivity, while minimally perturbing the sample [3]. Figure 1 presents the structure of the perfluorooctanesulfonic acid compound (PFOS).

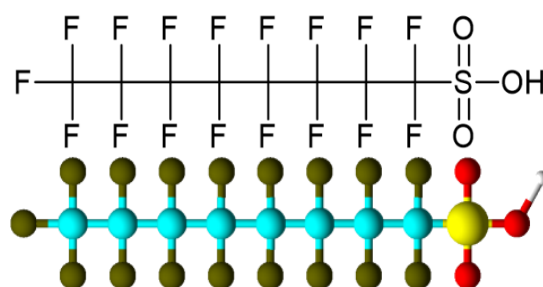


Fig. 1. Structural models of the PFOS molecule

In this experiment, powdered PVDF (poly(vinylidene fluoride)) was used to form the Fabry–Pérot interferometer cavity. The solvents were N,N-dimethylformamide (DMF) and chloroform. Polyvinyl butyral (Butvar) served as a cross-linking agent and adhesion promoter to the optical fiber. The sensor's sensitivity was evaluated using a chromatographic standard, perfluorooctanesulfonic acid (PFOS), in methanol (100 $\mu\text{g}/\text{mL}$, 95 % purity). A buffered oxide etch (BOE) solution ($\text{NH}_4\text{F}:\text{HF}$ 40 %) in a 6:1 ratio was used to prepare the fiber surface.

* E-mail: Patryk.Radek@polsl.pl



Weighed out: 1.70 g PVDF powder, 0.03 g Butvar, 14 mL DMF and 2 mL chloroform. Poured the DMF into a 25 mL beaker and heated it on a magnetic stirrer to 70 °C. Added the PVDF to the heated DMF; in a separate beaker, dissolved the Butvar in chloroform. Combined the two solutions, stirred, and covered the beaker to minimize solvent evaporation; continued heating for 1 h. After cooling to room temperature, transferred the solution into a dark, airtight bottle. Prepared an adhesion primer by dissolving Butvar in chloroform at a 1:10 ratio as an adhesion promoter.

Used standard single-mode optical fibers terminated with SC-APC pigtails. Stripped the protective coating with a fiber stripper and cleaned the fibers with a lint-free wipe soaked in isopropanol. Cleaved all fibers to the same length using a precision fiber cleaver. Etched the fiber end-faces in the BOE solution for 30 s, then rinsed thoroughly in ultrapure water. Dried the fibers in a fume hood until all moisture had evaporated.

Began the dip-coating process by applying five layers of primer. After each dip, we waited for complete solvent evaporation (monitored with a Yokogawa analyzer), dipping and withdrawing the fiber at 10 mm/s. Applied ten successive layers of the PVDF solution under the same dipping conditions. After coating, the fibers were left at 22 °C for 24 h to ensure full solvent evaporation and layer stabilization. Figure 2 of the fabricated Fabry–Pérot interferometric sensor: a standard single-mode fiber terminated with an SC-APC pigtail, its tip coated with a PVDF layer and housed in a protective sleeve, ready for immersion measurements.

Figure 3 illustrates the measurement setup used to verify the sensitivity of the Fabry–Pérot fiber-optic sensor to PFAS. Light source: a broadband Thorlabs SLD1550S-A2, emitting in the 1450–1650 nm range, coupled into the system via a standard optical fiber. Optical circulator: a three-port optical circulator that directs light from the input port to the sensor and, after reflection, routes it to the spectrum analyzer. Fabry–Pérot sensor: the fiber tip is coated with PVDF and immersed in the sample (water, PFOS solutions); the interferometric cavity responds to changes in refractive index and coating thickness by modulating the reflected spectrum. Spectrum analyzer: a Yokogawa AQ6370D records the position and contrast of the interference fringes over 1400–1650 nm; shifts in the fringe maxima indicate the sensor’s response to PFOS [4].

A thin PVDF layer is deposited on the tip of an optical fiber, forming a Fabry–Pérot interferometric cavity with the fiber end-face. Incident light is partially reflected at the fiber PVDF interface (I_1) and at the PVDF surrounding interface (I_2). These two reflected beams overlap and interfere, producing a sinusoidally modulated reflection spectrum whose resonance peaks and troughs satisfy [5].



Fig. 2. Photograph of the fabricated Fabry–Pérot fiber-optic sensor.

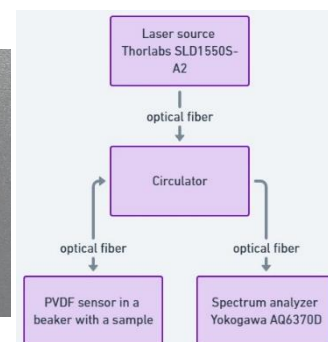


Fig. 3. Block diagram of the easurement system [4].

$$I(\lambda) = I_1 + I_2 + 2\sqrt{I_1 I_2} \gamma \cos\left(\frac{4\pi nL}{\lambda} + \phi_0\right), \quad (1)$$

where:

- I_1 and I_2 are the intensities reflected from the inner and outer surfaces
- γ is the coherence factor of the light source
- n is the refractive index of the PVDF layer
- L is the physical thickness of the PVDF layer
- λ is the free-space wavelength
- ϕ_0 is the initial phase offset

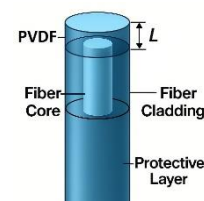


Fig. 4. Diagram of the Fabry–Pérot niche.

Adsorption of PFAS molecules (e.g., PFOS) onto the PVDF surface alters n and/or L , changing the optical path difference $\Delta(nL)$ and shifting the fringe positions in the reflected spectrum. By measuring the wavelength shift $\Delta\lambda$ of these fringes, the analyte concentration in the sample can be quantified.

To evaluate the sensor’s durability and measurement repeatability, six consecutive cycles of immersion in water (“WET”) and drying in air (“DRY”) were performed. In each cycle, the position of the central interference minimum in the 1580–1600 nm band was measured, and the shift was calculated as $\Delta\lambda = \lambda_{WET} - \lambda_{DRY}$. The average shift—shown in Figure 5 as the “Dry (avg)” and “Wet (avg)” curves—was 5.09 nm (SD = 0.7 nm), confirming the high repeatability and optical stability of the PVDF coating over multiple wet–dry cycles.

Cycle	Dry λ_c (nm)	Wet λ_c (nm)	$\Delta\lambda$ (nm)
1	1586.84	1591.20	4.36
2	1587.12	1593.60	6.48
3	1587.68	1593.00	5.32
4	1588.28	1593.40	5.12
5	1587.76	1592.40	4.64
6	1587.92	1592.56	4.64
Mean	1587.60	1592.69	5.09

Table 1. Measured interference minimum wavelengths (λ_c) and resulting shifts ($\Delta\lambda$) for six consecutive dry (air) and wet (water) cycles.

The consistent 5.09 nm shift, clearly visible in the averaged curves, demonstrates that the PVDF layer maintains its optical and mechanical properties through repeated the wet–dry cycles, which is critical for field deployment and long-term monitoring.

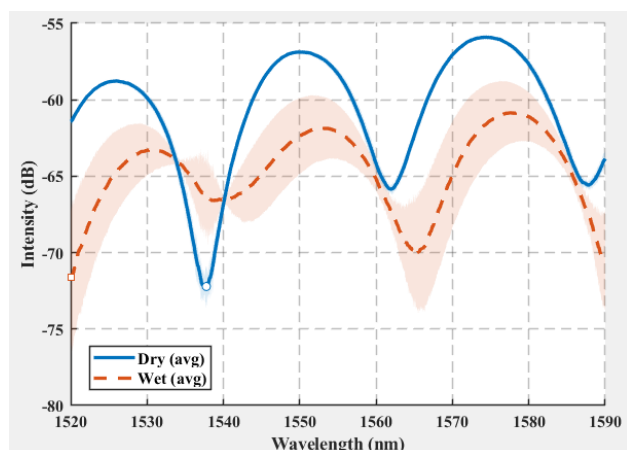


Fig. 5. Averaged Fabry–Pérot reflection spectra of the PVDF-coated fiber under dry and wet conditions, with shaded bands indicating ± 1 SD.

Figure 6 shows the interferometric spectra of the PVDF–FPI sensor at four key stages: dry baseline, PFOS START, PFOS END, and post-detoxification. Upon PFOS addition, the interference minimum red-shifts by $\Delta\lambda = 5.9$ nm (from PFOS START to PFOS END). After rinsing, it returns to within 0.4 nm of its original position. Because this 5.9 nm shift greatly exceeds the ~ 0.7 nm variability observed during wet–dry cycling, it demonstrates the sensor’s high sensitivity to PFOS. Although the spectral shape after detoxification differs slightly from the initial dry baseline, the position of the minimum recovers almost fully, confirming a largely reversible response and the sensor’s potential for regeneration under field conditions.

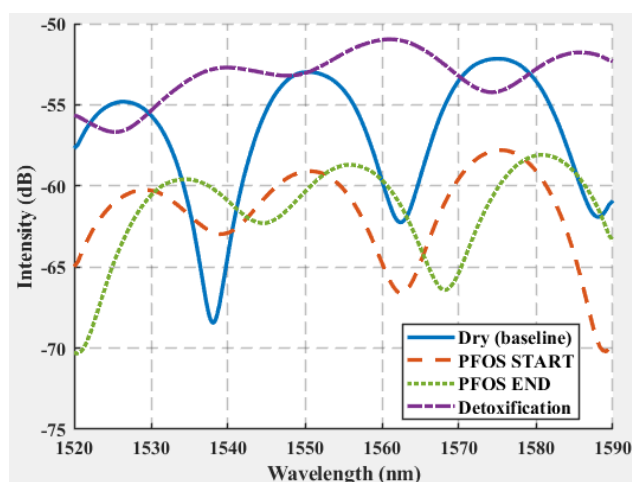


Fig. 6. Overlaid interferometric spectra of the PVDF-coated FPI during the cycles, showing reversible response with minor spectral variation after detoxification.

In conclusions, the developed PVDF-coated fiber-optic Fabry–Pérot interferometer demonstrated:

- Repeatable interferometric response over wet–dry cycles ($\Delta\lambda = 5.09$ nm, SD = 0.7 nm, RSD $\approx 13.8\%$), despite moderate variation between cycles
- Detectable spectral response to PFOS at 10 $\mu\text{g/mL}$ ($\Delta\lambda = 5.9$ nm), suggesting potential for further sensitivity improvements
- Reversible adsorption behavior, with partial spectral recovery after rinsing (shift < 0.4 nm).

Thanks to its simple dip-coating fabrication, low material cost, and portable design, the sensor shows promise for in-field PFAS detection. Future work will focus on determining the detection limit (LOD), optimizing PVDF layer thickness, and incorporating nanostructures to enhance selectivity, along with temperature compensation to ensure stability under variable environmental conditions. While the current approach enables PFOS detection, its selectivity remains limited and will be improved through surface functionalization in future studies.

References

- [1] *Carbon–Fluorine Bond Strength*, Alfa Chemistry Fluoropolymers Resource, <https://fluoropolymers.alfa-chemistry.com/resources/carbon-fluorine-bond.html>.
- [2] Z. Abunada, S. Safi, A. Ahmad, M.M.F. Chitta, *Water* **12**(12), 3590 (2020), doi: 10.3390/w12123590.
- [3] C.F. Kwiatkowski, M.L. Cannon, D.T. Hoffman, J.A. Buck, S.A. Fedorak, *Environ. Sci. Technol. Lett.* **7**(8), 532 (2020), doi: 10.1021/acs.estlett.0c00255.
- [4] P. Radek, K. Barczak, A. Olszewska, Optical fiber sensor for per- and polyfluoroalkyl substances (PFAS) in *Proc. Integrated Optics – Sensors, Sensing Structures and Methods, IOS’2025, Szczyrk, Poland*, Feb. 24–28, 2025, p. 81.
- [5] F. Faiz, S.J. Mihailov, D. Thapa, V. Kayunkid, G. Viney, *Sens. Actuators B Chem.* **312**, 128006 (2020), doi: 10.1016/j.snb.2020.128006.